

University of New Hampshire
University of New Hampshire Scholars' Repository

Honors Theses and Capstones

Student Scholarship

Spring 2018

Characterization of Palmitoyltransferase Proteins in *Arabidopsis thaliana*

Danielle McGinty

University of New Hampshire, Durham, danielle.mcginity32@gmail.com

Follow this and additional works at: <https://scholars.unh.edu/honors>

 Part of the [Plant Biology Commons](#)

Recommended Citation

McGinty, Danielle, "Characterization of Palmitoyltransferase Proteins in *Arabidopsis thaliana*" (2018). *Honors Theses and Capstones*. 427.

<https://scholars.unh.edu/honors/427>

This Senior Honors Thesis is brought to you for free and open access by the Student Scholarship at University of New Hampshire Scholars' Repository. It has been accepted for inclusion in Honors Theses and Capstones by an authorized administrator of University of New Hampshire Scholars' Repository. For more information, please contact nicole.hentz@unh.edu.

Danielle McGinty

Spring 2018

Honors Senior Thesis

Characterization of Palmitoyltransferase Proteins in *Arabidopsis thaliana*

Introduction

Protein palmitoylation or S-acylation is the reversible, covalent, post-translational lipid modification of cysteine residues with palmitate or sometimes stearate¹. Protein S-acyl transferases (PATs) catalyze this reaction. PATs are a family of integral membrane proteins with four to six transmembrane domains and a conserved cytoplasmic Asp-His-His-Cys (DHHC) Cysteine-rich (Cys-rich) motif that is thought to be essential for enzymatic activity². S-acylation increases the lipophilicity of the modified protein, which may promote membrane association or allow relocation of the acylated integral membrane protein (i.e., into lipid rafts). S-acylation can affect protein trafficking between membranes, influence protein stability, modulate protein function, or mediate interaction of the acylated protein with other proteins¹. The reversibility of S-acylation enables a large amount of control over the processes that this modification regulates³.

PAT proteins are found throughout eukaryotes, ranging from yeast (*Saccharomyces cerevisiae*), where they were first described, to humans. There are 7 DHHC-Cys-rich domain proteins in yeast, 24 in mice, and 23 in humans. Human *DHHC* genes are implicated in numerous disorders including cancers and neural diseases like schizophrenia and Huntington's disease⁴. S-acylation influences cell size, growth, and polarity within many eukaryotic cells²; however, knowledge of the roles of S-acylation in plant cells is limited in comparison to other organisms.

The model plant *Arabidopsis thaliana* used in this study has twenty-four *PAT* genes. *Arabidopsis* is an effective model organism because it is small and has a fully sequenced genome, available genomic resources, high fecundity, a short life cycle, and prolific seed production⁵. The *PAT* loci in *Arabidopsis* are found on multiple chromosomes. Chromosome 3 contains ten *PAT* loci, chromosomes 4 and 5 each

contain five loci, three loci are found on chromosome 2, and only *PAT22* is found on chromosome 1¹.

PAT genes in *Arabidopsis* are grouped into three main clades (A, B, and C) with different levels of conservation¹. Overall, the *PAT* protein family has a relatively low level of sequence conservation because each of the three clades evolved at different times. It is likely that Clade A evolved later than Clades B and C due to the higher level of sequence conservation between the members of Clade A¹.

Most *PATs* in *Arabidopsis* are expressed in many tissues and are expressed throughout development, whereas a subset of *PAT* genes exhibit very high expression, primarily in pollen and stamens¹. The size of the *PAT* gene family (24) and diversity of expression indicates that there are likely a large number of targets for this lipid modification. Indeed, more than 600 palmitoylated proteins are predicted in *Arabidopsis*⁶. One *PAT* expressed preferentially in pollen has been shown to be required for pollen development⁷ and this may also be true for other *PATs* expressed highly in flowers and stamen¹.

Palmitoylation of proteins in plants can occur at the Golgi, plasma membrane, endosomal compartments, vacuolar membrane, or the endoplasmic reticulum¹. Most *Arabidopsis* *PAT* proteins are found in the plasma membrane. In yeast, three *PATs* are localized at the endoplasmic reticulum, two at the Golgi, and one at the vacuole and plasma membrane. In human, *PATs* are localized at the Golgi, endoplasmic reticulum, and plasma membrane⁸. This observation indicates that S-acylation may be functionally different in plants than in mammals and *S. cerevisiae*.

This study used *Arabidopsis* to characterize *PAT* mutants, which were obtained from various companies or academic institutions that have produced collections of T-DNA insertion mutants. The focus of this study was predominantly on the characterization of *PAT3*, but also involves *PAT16*. SALK T-DNA mutants in *PAT3* (At5g05070) were ordered by our lab and genotyped. A previous student (Judy Hoskin) identified homozygous *pat3-2* and *pat3-3* mutants.

The goal of this study was to establish whether *pat3-2* and *pat3-3* were loss-of-function mutants in preparation for using them to infer the normal function of *PAT3*. T-DNA mapping was used to characterize the T-DNA insertion in these mutants, and the junction between *PAT3* and the T-DNA border was sequenced to confirm the location of the T-DNA insertion and infer the effect of the insertion on *PAT3* gene function. RNA collected from *pat3-2* was reverse transcribed into cDNA. RT-PCR was used to detect mRNA transcripts and to deduce whether the mutant was likely to produce any functional protein. Plants transformed with *PAT3-GUS* constructs were used to determine gene expression, which helped to clarify when in the plant's life cycle to collect RNA for mRNA transcript detection. As a side project, a *PAT16-GUS* fusion construct was made to deduce *PAT16* gene expression in the future. Studying the function of *PATs* using various *PAT* mutants in *Arabidopsis* will give us more insight into protein S-acyl transferases and their importance in plants.

Methods

Sterile Growth of *Arabidopsis*

One mL of 70% ethanol and one drop of 10% Triton X-100 were added to approximately 50 seeds under sterile conditions. The sample was gently agitated for 5 minutes, then seeds were allowed to settle. The liquid was replaced with 1 mL of 100% ethanol and one drop of Triton X-100 and agitated gently again for 5 minutes. The liquid was replaced with 1 mL of 100% ethanol and agitated for 5 minutes. After the ethanol was removed, seeds were air-dried under sterile conditions. Dried seeds were added to 20 mL of sterile Low Sucrose Medium (0.5X Murshige-Skoog Medium Plus Gamborg's vitamins [Caisson Laboratories, Catalog Number: MSP0506], 1% Plant Culture Grade I sucrose [Sigma, St. Louis, MO], pH 5.7-.5.8 using KOH). Cultures containing seeds were agitated gently (164 rpm) at 25°C with a 12-h photoperiod for 2 weeks.

Isolation of DNA

DNA was isolated from 100 mg of plant tissue following the protocol for the DNeasy Plant Mini Kit (Qiagen, Valencia, CA). DNA was eluted with 100 µL of nuclease-free water.

PCR DNA Cleanup

PCR cleanup was performed using Monarch PCR DNA Cleanup Kit (New England Biolabs, Ipswich, MA) according to manufacturer's instructions.

Rapid DNA Extraction from *Arabidopsis thaliana*

DNA was extracted using a published method⁹. Briefly, leaf pieces (5 mm²) were mixed with 40 µL of 0.25 N NaOH and the leaf was punctured to damage the tissue. The sample was boiled for 30 seconds. 40 µL of 0.25 N HCl was added, followed by 20 µL of 0.5 M Tris-HCl, pH 8 containing 0.25% Nonidet P-40 (Sigma). The sample was boiled for 2 minutes. DNA preps were stored at 4°C.

PCR for Genotyping and Amplification of Desired PAT DNA Segments

Reactions contained 0.2 mM dNTPs, 1X homemade Taq buffer (20 mM Tris-Cl, pH 8, 1 mM DTT, 0.1 mM EDTA, 100 mM KCl, 0.5% Nonidet P40, 0.5% Tween 20, 50% glycerol, 0.2 mg/mL bovine serum albumin), 0.2 µM of each primer (Table 1), and 0.3 µL homemade Taq DNA polymerase. For plasmid DNA, 5-100 ng of DNA template was used, whereas 0.1-2 µg was used for genomic DNA templates. The PCR profile included an initial denaturation step of 94°C for 2 minutes, followed by 35 cycles of 94°C for 30 seconds, the calculated annealing temperature (Table 2) for 30 seconds, and 72°C for 1-2 minutes.

Gel Electrophoresis

Either 1% or 1.5% agarose gels were used. Samples were mixed with 0.3-0.5 µL of loading dye (15% Ficoll [type 400], 0.25% bromphenol blue, 0.25% xylene cyanol). Size standard was 1 Kb Plus DNA Ladder (Invitrogen, Carlsbad, CA). DNA was detected using 0.5-1 µg/mL ethidium bromide.

Table 1. Primers used in this study.

Primer Name	Sequence (5' → 3')	Location	Function
DHC15-5'	GAT CAC CAT TGT CCA TGG GTT GGT	forward primer in <i>PAT3</i> 1 st exon upstream of <i>pat3-2</i> and <i>pat3-3</i> T-DNA insertion sites	T-DNA Mapping
DHC15-3'	ACT TGG GCA AGT CTA GTT GAG ATG	reverse primer in <i>PAT3</i> 3 rd exon downstream of <i>pat3-2</i> and <i>pat3-3</i> T-DNA insertion sites	T-DNA Mapping
JMLB1-S	GTT GCC CGT CTC ACT GGT G	primer faces out the left border of T-DNA lines from Salk Institute	T-DNA Mapping
RB	CGC AAT AAT GGT TCC TGA CGT A	primer faces out the right border of T-DNA lines from Salk Institute	T-DNA Mapping
PAT3-A	CTT GCT TGC TCT ATC GTC	forward primer in 2 nd exon of <i>PAT3</i>	RT-PCR
PAT3-B	ATA GCT TCC CAG GTT GTC	reverse primer in 3 rd exon of <i>PAT3</i>	RT-PCR
PAT3-C	GGA GGA CAA TGT CTG ATG	forward primer in 3 rd exon of <i>PAT3</i> upstream of T-DNA insertion site	RT-PCR
PAT3-D	GAG ATC TAG TTG CGA AGG	reverse primer in 4 th exon of <i>PAT3</i> downstream of T-DNA insertion site	RT-PCR
PAT3-E	ATA CCT CCT CCG TGA GAT AC	forward primer in 4 th exon of <i>PAT3</i>	RT-PCR
PAT3-F	TGG GCA AGT CTA GTT GAG	reverse primer in 4 th exon of <i>PAT3</i>	RT-PCR
PAT16-C	CTC TAC TTT GGT TGT CGC ACT TAC	forward primer in PAT16 “promoter”, 1210 bases before translation start	TOPO Cloning
pPAT16 reverse	ATG TTT TGT TTC AGA TGA ATC AGG	reverse primer that ends at last amino acid codon in <i>PAT16</i>	TOPO Cloning

Table 2. Primer pairs and conditions used for PCR .

Forward Primer	Reverse Primer	Annealing temperature	Elongation Time
DHC15-5'	DHC15-3'	68°C	2 minutes
DHC15-5'	JMLB1-S	62°C	2 minutes
DHC15-3'	JMBL1-S	62°C	2 minutes
DHC15-5'	DHC15-5'	68°C	2 minutes
DHC15-3'	DHC15-3'	68°C	2 minutes
JMLB1-S	JMLB1-S	62°C	2 minutes
JMLB1-S	RB	62°C	2 minutes
DHC15-5'	RB	62°C	2 minutes
DHC15-3'	RB	62°C	2 minutes
RB	RB	62°C	2 minutes
PAT3-A	PAT3-B	49°C	1 minute
PAT3-C	PAT3-D	49°C	1 minute
PAT3-E	PAT3-F	49°C	1 minute
PAT16-C	pPAT16 reverse	62°C	2 minutes

RNA and DNA Quantitation

RNA and DNA were quantitated using the Qubit fluorometer (Invitrogen) following the manufacturer's instructions.

DNA-Free RNA Isolation

20-30 mg of 2-week-old seedlings, 4-week-old seedlings, siliques, or a combination of flower buds and open flowers were frozen using liquid nitrogen and ground to a fine powder. The frozen, ground tissue was quickly added to 300 μ L of cell lysis solution (2% SDS, 68 mM sodium citrate, 132 mM citric acid, 1 mM EDTA). The sample was vortexed for 2 seconds and incubated at room temperature for 5 minutes. 100 μ L of protein-DNA precipitation solution (4 M NaCl, 16 mM sodium citrate, 32 mM citric acid) was added to the cell lysate. The sample was mixed gently and incubated at 4°C for 10 minutes, then centrifuged at 4°C for 10 minutes. All centrifugations were carried out at top speed. 300 μ L of isopropanol was added to the supernatant. The sample was mixed by inversion and centrifuged for 4 minutes. The pellet was washed with 70% ethanol and dried. RNA was resuspended in 25 μ L distilled water (RNase free). 1X RQ1 DNase buffer and 2 μ L of RQ1 DNase I (Promega, Madison, WI) were added. The sample was incubated for 30 minutes at 37°C, then 1 μ L DNase stop was added before heat inactivating the DNase for 10 minutes at 65°C. 50 μ L of 7.5 M NH₄Ac and 400 μ L of 100% ethanol were added and the sample was centrifuged for 20 minutes at 4°C. The pellet was washed with 70% ethanol. The RNA was dried, resuspended in 20 μ L RNase-free water, and stored at -80°C.

Reverse Transcription Using Super Script IV

First strand cDNA synthesis was performed on RNA from 2-week-old seedlings, 4-week-old-seedlings, siliques, and flowers. For primer annealing, 2.5 µg anchored oligo dT primer (Invitrogen) and 5 µg of RNA were mixed with 1 µL of 10 mM dNTPs and brought to 13 µL. The sample was heated at 65°C for 5 minutes, then quickly transferred to ice for 1 minute. The reverse transcription reaction contained the 13 µL primer annealing reaction in a 1.7 mL tube, 1X first strand buffer (Invitrogen), 5 mM DTT, 40 U RNasin (Promega), and 200 U SuperScript IV Reverse Transcriptase (Invitrogen). The reaction was incubated for 60 minutes at 50°C. The reverse transcriptase was inactivated at 70°C for 15 minutes. cDNA was stored at -20°C.

PAT16-GUS Construct

PCR

PCR was performed to amplify *PAT16* genomic DNA from the *PAT16* promoter to its last codon before the stop codon using *PAT16-C* and *pPAT16* reverse primers and Q5 high fidelity 2X master mix DNA polymerase (New England Biolabs).

Addition of 3' A Overhangs

The reaction contained 1X homemade Taq buffer, 0.33 µM of dATPs, and 0.5 µL of homemade Taq DNA polymerase, and 638 ng purified PCR product in a final volume of 15 µL. The sample was incubated for 20 minutes at 72°C.

TOPO Cloning

4 μL of PCR product with 3' A overhangs was mixed with 1 μL of salt solution and 1 μL of the pCR8/GW/TOPO vector (Invitrogen). The TOPO cloning reaction was incubated at room temperature for 30 minutes.

DNA Sequencing

DNA sequencing was performed by Genewiz (South Plainfield, New Jersey).

Gateway Cloning to pGWB203

pGWB203 is a Gateway destination vector that contains the *HPT* hygromycin resistance gene, the *CAT* chloramphenicol acetyl transferase resistance gene, and a promoterless *GUS* β -glucuronidase reporter gene - all located between T-DNA left and right borders¹⁰. 150 ng of supercoiled pGWB203 (with *attR* sites) was added to 100 ng of supercoiled PAT16-TOPO plasmid (with *attL* sites) and brought to a total volume of 9 μL using TE buffer (1 mM EDTA, 10 mM Tris-Cl, pH 8). 1 μL of LR Clonase (Invitrogen) was added and the reaction was incubated at 25°C for one hour. After incubation, 1 μL of Proteinase K (Invitrogen) was added for 10 minutes at 37°C to remove the LR Clonase.

Electroporation

40 μL of electrocompetent *E.coli* TOPO10 cells or *Agrobacterium tumefaciens* GV3101 cells was added to plasmid DNA in a sterile 1-mm gap cuvette. After electroporation at 18,000 V/cm, 500 μL of SOC growth medium (2% Bacto-tryptone, 0.5% yeast extract, 10 mM NaCl, 2.5 mM KCl, 10 mM MgCl₂, 10 mM MgSO₄, and 20 mM glucose) was added immediately. For *E. coli*, the culture was incubated for one hour at 37°C with agitation, and for *Agrobacterium*, at 28°C for 4 hours. The cultures were spread on LB plates (1% Bacto-tryptone, 0.5% yeast extract, 0.17 M NaCl) containing either 100

µg/mL spectinomycin to select for colonies containing the PAT16-TOPO plasmid or 50 µg/mL kanamycin to select for PAT16-GWB203 colonies. Cultures were incubated overnight at 37°C for *E. coli* or at 28°C for 2-3 days for *Agrobacterium*.

Plasmid Purification

Individual *E. coli* colonies were inoculated in LB broth with antibiotic (kanamycin [50 µg/mL] or spectinomycin [100 µg/mL]) and incubated overnight at 37°C with strong agitation. Plasmid purification was performed using Monarch Plasmid Miniprep Kit (New England Biolabs). Plasmid DNA was eluted with 30 µL of nuclease-free water heated to 50°C prior to the elution to increase yield if necessary.

Restriction Digestion

Restriction digestion was performed on purified plasmid DNA. 10 µL digests containing 0.2 µL of restriction enzyme, 1X restriction enzyme buffer, and 66-250 ng of plasmid (depending on restriction enzyme) were incubated at 37°C for one hour. The digests were analyzed using gel electrophoresis with a 1.5% agarose gel.

Arabidopsis Transformation

Agrobacterium tumefaciens GV3101 cells carrying the PAT16/GWB203 plasmid were grown overnight in LB broth containing 50 µg/mL kanamycin at 28°C with agitation. The cells were centrifuged at 5000 x g for 5 minutes. The pellet was resuspended in 50 mL of resuspension buffer (5% sucrose and 0.05% Silwet [Lehle Seeds, Round Rock, Texas]). The concentration was adjusted with additional resuspension buffer to optical density 0.6-0.8 at 600 nm. Flowers of wildtype *Arabidopsis thaliana* Columbia-0 were dipped in the *Agrobacterium* suspension for about 10 seconds. The plants were kept in high humidity conditions overnight. The next day, the plants were rinsed with cool water

to remove sucrose. Plants were placed in the growth room (18h photoperiod; 21°C) until seeds were harvested.

GUS Histochemical Assay

50 mL of GUS assay solution¹¹ was made using 0.1 M NaPO₄, 1 mM of both potassium ferricyanide and potassium ferrocyanide, 0.01 M EDTA, 1000 µL of Triton X-100, and 25 mg/mL X-Gluc (Rose Scientific, Edmonton, Alberta). (X-Gluc was dissolved in dimethylformamide before adding to the GUS assay solution.) Plant tissue was submerged in GUS assay solution and vacuum infiltrated for 5 minutes, then incubated at 37°C for 7-24 hrs, depending on the assay. Tissue was decolorized with 95% ethanol, then through a stepwise series of 70% ethanol, 50% ethanol, water to transition the tissue back to aqueous conditions. Samples were mounted in water for microscopy.

Results

T-DNA Mapping of *pat3-2* and *pat3-3*

T-DNA mapping uses PCR to characterize the number of T-DNAs at the insertion site, the structure and orientation of the T-DNA, and the gain or loss of DNA at the site of insertion. In the hypothetical T-DNA insertion (Figure 1), we would not expect a PCR product from genomic primers DHC15-5' and DHC15-3' because they flank the large T-DNA insert. We would expect a product from JMLB1-S and DHC15-5' that confirms that the left border in the T-DNA, which binds JMLB1-S, faces upstream. We would also expect a product from RB and DHC15-3', which would confirm that there is a right border in the T-DNA facing downstream.

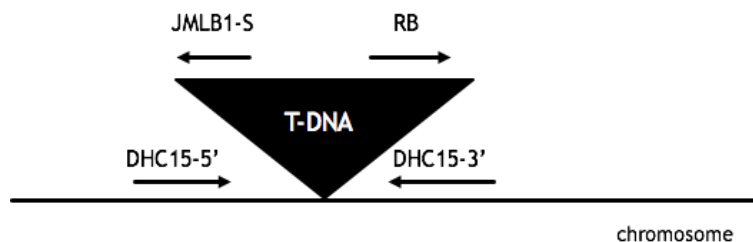
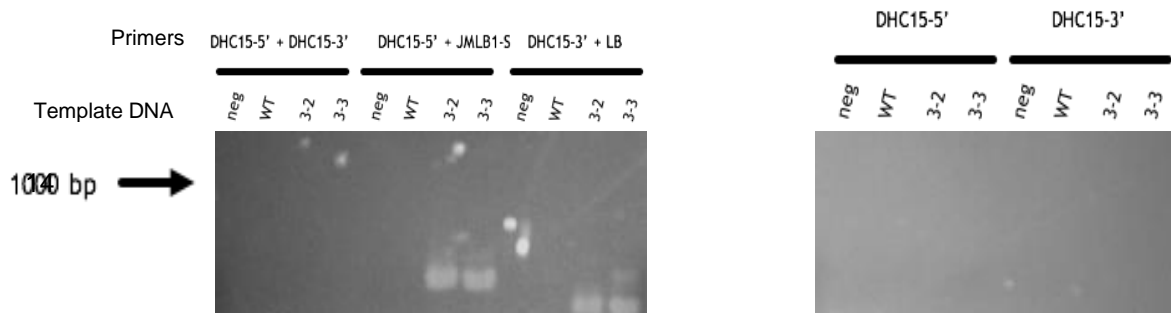


Figure 1. Structure of a theoretical T-DNA insertion showing locations of primers that produced PCR products during T-DNA mapping.

For *pat3-2* (SALK_074034) and *pat3-3* (SALK_122426) mutants, PCR was performed with two T-DNA primers (JMLB1-S and RB) and two *PAT3* gene-specific primers (DHC15-5' and DHC15-3') in all possible combinations (Tables 1 and 2; Figure 2). PCR products were generated with DHC15-5' and JMLB1-S, as well as with



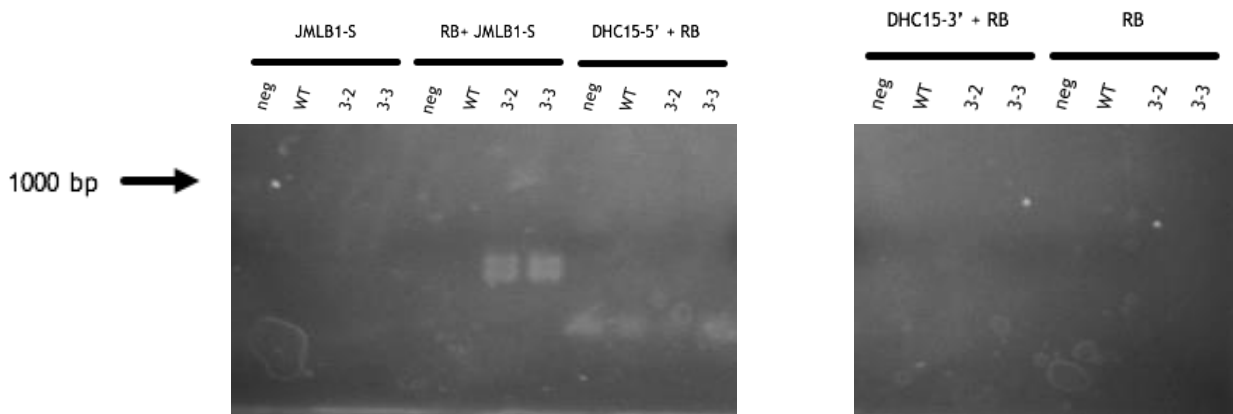


Figure 2. PCR products from T-DNA mapping of *pat3-2* and *pat3-3*. PCR was performed using all combinations of *PAT3* genomic (DHC15-5' + DHC15-3') and T-DNA (JMLB1-S + RB) primers in order to characterize the T-DNA insertion. neg = negative control; WT = wildtype Col-0 genomic DNA; 3-2 = *pat3-2* genomic DNA; 3-3 = *pat3-3* genomic DNA; LB = JMLB1-S.

DHC15-3' and JMLB1-S, indicating that the T-DNA has left borders on each end (Figures 2 & 3A). Sequencing of these PCR products revealed a 76 basepair deletion immediately upstream of the T-DNA insertion site. PCR product with JMLB1-S and RB indicates one or more internally-facing right and left borders of unknown orientation, indicating the presence of multiple T-DNAs at the insertion site. Primers DHC15-5' and DHC15-3' did not initially give a product when genomic wildtype DNA was used as template but a repeat reaction did have the expected sized product (data not shown), indicating that the primers were functioning properly. Due to their similar product sizes

and identical T-DNA/genomic junction sequences, we concluded that *pat3-2* and *pat3-3* were the same allele.

The T-DNA begins at the first codon of the fourth exon, which corresponds to the cytosolic tail of *PAT3*, after the fourth transmembrane domain (Figure 3B). This area contains several regions that are conserved across Clade A (*PAT1* through *PAT9*) proteins, including NxoTTxE and NPY motifs¹. NPY is proposed to be required for enzymatic activity¹. Although a T-DNA insertion at the beginning of the *PAT3* coding region would perhaps be more likely to create a knockout mutant, the mutation in *pat3-2/pat3-3* in the cytosolic tail has the potential to destabilize or inactivate the protein. In addition, because the SALK T-DNA left border contains an outward-facing 35S promoter¹², antisense *pat3* RNA may be synthesized which could hybridize to the sense *pat3* mRNA and trigger RNA interference and gene silencing.

pat3-2 mRNA Transcript Detection

To determine the presence of *pat3* transcript during plant development, tissue was isolated from multiple stages of the *Arabidopsis* lifecycle for RNA extraction. We arbitrarily chose one of the *pat3* mutants for mRNA transcript detection, because *pat3-2* and *pat3-3* appeared to be the same allele based on T-DNA mapping.

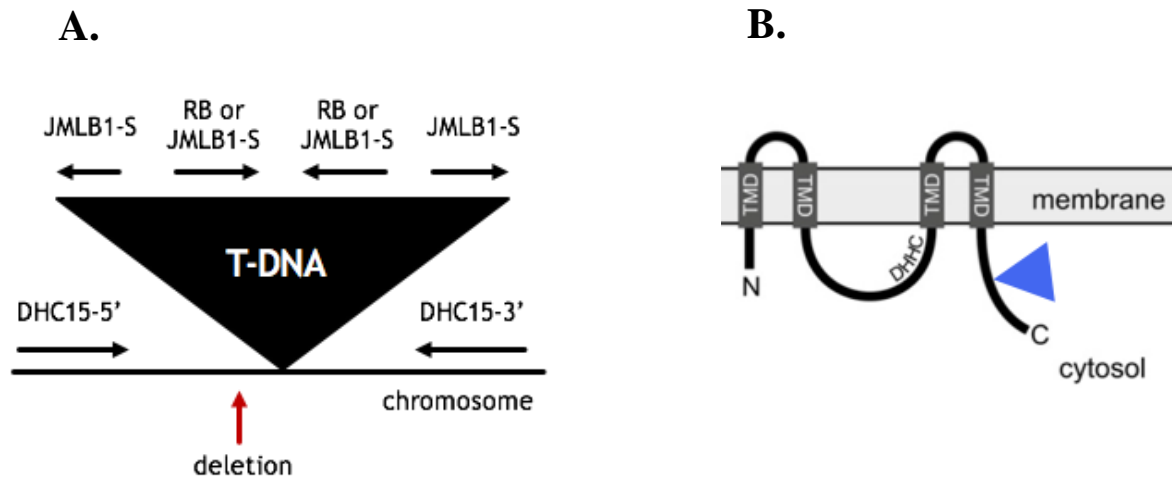


Figure 3. Schematic of *pat3-2* T-DNA insertion based on T-DNA mapping and sequencing. A) Simplest interpretation of the structure of the T-DNA in *pat3-2* and *pat3-3* mutants. B) The location of *pat3-2* and *pat3-3* T-DNA insertion in the cytosolic tail, after the fourth transmembrane domain. T-DNA is in blue. (figure modified from www.intechopen.com)

RNA was isolated from the following tissues from *pat3-2* mutants: 2-week-old seedlings, 4-week-old seedlings, siliques, and flowers which consisted of the cluster of buds and flowers at the top of the inflorescence stem (Table 3). In lieu of wildtype RNA, RNA from *pat16-3* mutants isolated at the same developmental stages was used as the positive control (Table 3). The mRNA from the *pat3-2* and *pat16-3* samples was reverse transcribed into cDNA. The cDNA was used as a template for PCR. Whenever possible, primers were located in different exons to distinguish PCR products generated from genomic DNA contamination of samples vs. cDNA products. Three primer pairs were used to amplify the *PAT3* cDNA. Primers PAT3-A and PAT3-B (referred to as A+B in tables and figures) were upstream of the T-DNA insertion site and spanned an intron, PAT3-C and PAT3-D flanked the T-DNA insertion site and spanned an intron, and PAT3-E and PAT3-F were located downstream of the T-DNA but did not span an intron (Tables 1, 2 & 4; Figure 4). Wildtype Columbia-0 genomic DNA was used as a template

with each primer pair to determine the size of the product that would be generated if there was genomic DNA contamination of the RNA samples.

Table 3. Concentration of *pat16-3* (positive control) and *pat3-2* RNA samples.

	<i>pat16-3</i>	<i>pat3-2</i>
2-week-old seedlings	1008 ng/μL	200 ng/μL
4-week-old seedlings	976 ng/μL	198 ng/μL
Siliques	40.4 ng/μL	62.2 ng/μL
Flowers	272 ng/μL	752 ng/μL

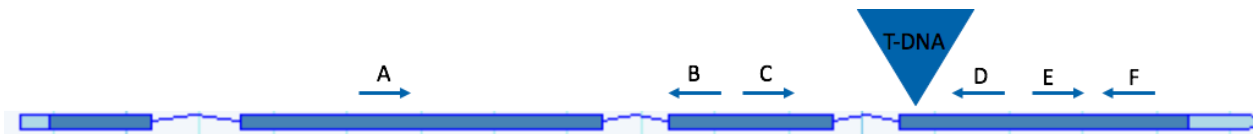
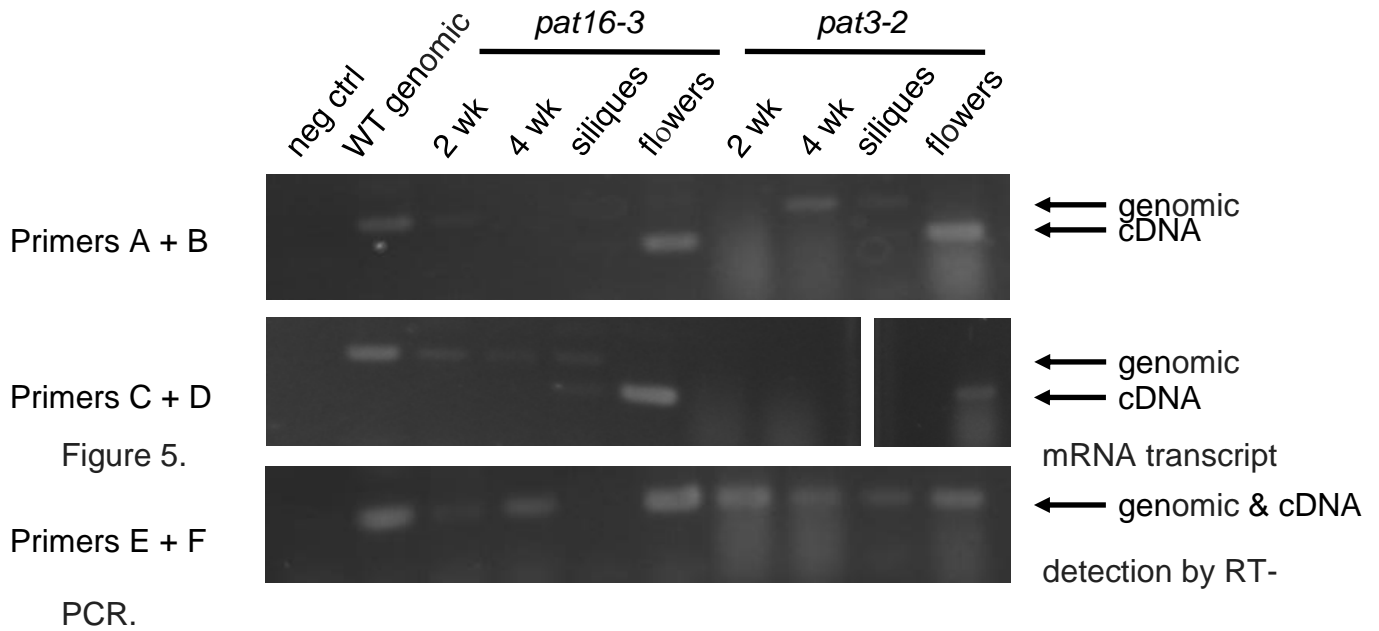


Figure 4. Location of primers for RT-PCR in *PAT3* gene in relation to the T-DNA insertion site. light blue boxes = untranslated regions; dark blue boxes = coding regions; lines = introns; arrows = primers.

Table 4. Expected RT-PCR product sizes.

Primer Pairs	Genomic product	Expected cDNA product (wildtype)	Observed cDNA product (wildtype)	Expected cDNA product (<i>pat3</i>)	Observed cDNA product (<i>pat3</i>)
A + B	305 bp	213 bp	~200 bp (flowers only)	No product	~200 bp (flowers only)
C + D	328 bp	236 bp	~260 bp (flowers only)	No product	~260 bp (flowers only)
E + F	198 bp	198 bp	inconclusive	No product	inconclusive



For primers A+B and primer C+D, cDNA-sized products were detected only in flowers and not in 2- or 4 week-old seedlings or in siliques. There is evidence of genomic DNA contamination in 2- and 4 week-old seedlings and siliques of both *pat3-2* and *pat16-3* mutants. Since the *pat16-3* mutants have a wildtype *PAT3* gene, the *pat16-3* results indicate that most *PAT3* transcription is in flowers. In addition, product from A+B primers in *pat3-2* is not unexpected because the T-DNA is in the cytosolic tail of *PAT3*, so upstream transcript is likely being made from the native *PAT3* promoter. However, transcript from primers C+D in *pat3-2* flowers indicates that mRNA spanning the T-DNA insertion site is being produced; the simplest explanation for this result is that the *pat3-2* mutant plants were not homozygous. We would not expect a product from primers C+D because they flank the T-DNA insertion site. The expected product sizes from cDNA and genomic templates are the same for primers E+F because the

primers do not span an intron. Because primer pairs A+B and C+D showed evidence of genomic DNA contamination in most samples, we could not draw conclusions based on the E+F primer pair. However, in the flowers, where we haven't observed genomic DNA contamination, a product was amplified with primers E+F. This indicates either that *PAT3* transcript downstream of the T-DNA is being produced, perhaps by the 35S promoter near the left border, or that the mutants are heterozygous.

PAT3-GUS Histochemical Assays

Histochemical GUS assays were done on wildtype *Arabidopsis thaliana* Colombia-0 plants that had been transformed previously with the PAT3-GUS construct made by BMCB 754 class in Fall 2015. Transformants were selected for hygromycin resistance and genotyped to confirm presence of the transgene. The *PAT3* genomic fragment that was fused to the GUS (β -glucuronidase) gene contained 989 bp upstream of the *PAT3* start codon and is expected to contain sufficient *PAT3* regulatory sequences to result in authentic gene expression. The construct also contained all introns and exons up to the final codon of the open reading frame. The *uidA* or *GUS* gene encodes β -glucuronidase (GUS), an enzyme activity lacking in *Arabidopsis* that can be easily detected *in planta* using a histochemical assay. Thus, when *PAT3* is transcribed and translated, the protein produced will be fused in-frame with the GUS protein. GUS cleaves X-Gluc to create a blue product in cells where *PAT3* is expressed. Tissue from plants transformed with T-DNA carrying PAT3-GUS hybrid gene was submerged in GUS assay solution. In preliminary GUS assays, *PAT3* expression was shown in the anthers of *Arabidopsis*, most likely in the pollen (Figure 6).

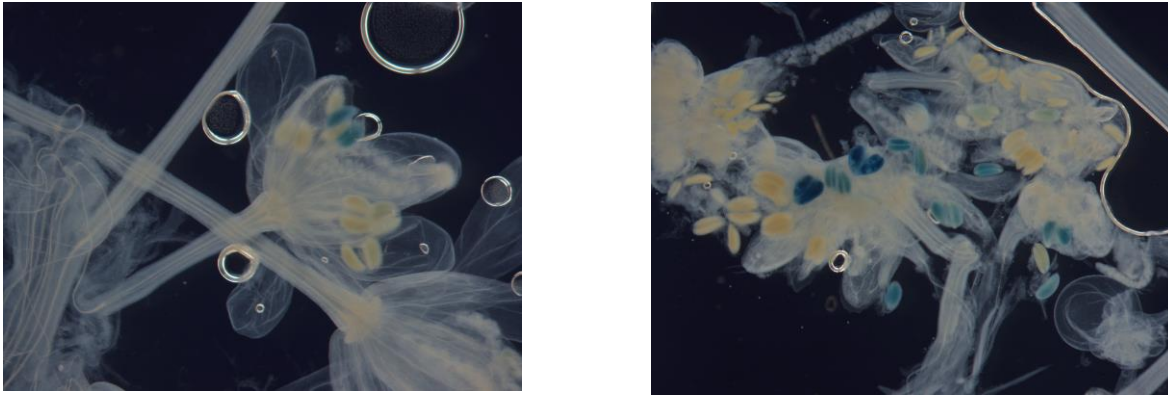


Figure 6. *PAT3* expression in anthers of *Arabidopsis thaliana* detected with a GUS histochemical assay.

PAT16 cloning

Characterizing expression of *PAT* genes helps us to understand when our genes of interest are expressed, to determine where and when to collect samples for mRNA transcript detection, and to conjecture where mutant phenotypes are likely to be found. To observe *PAT16* gene expression, a plasmid that expresses a *PAT16-GUS* hybrid gene was made.

The PCR product was amplified using PAT16-C, a forward primer located 1210 bp upstream of the *PAT16* translation start site and located in the 7th exon of the upstream gene (At3g09330), and pPAT16 reverse, which ends after the last amino acid codon of *PAT16* (At3g09320). The *PAT16* PCR product was the expected size (3179 bp; Figure 7) and was purified and quantitated (73.8 ng/uL). After adding 3' A overhangs, the *PAT16* product was ligated into pCR8/GW/TOPO by TOPO cloning. The pCR8/GW/TOPO contains *attL1* and *attL2* sites for subsequent Gateway cloning of the

gene of interest into a destination vector, primer binding sites for DNA sequencing, and the spectinomycin resistance gene for selection in *E. coli*.

Cloning products were transformed into electrocompetent *E. coli* and transformants were selected on spectinomycin plates. Plasmids were purified from three transformants and quantified at 123.6 ng/uL, 172.4 ng/uL, and 112 ng/uL. Restriction digestions using EcoRV were used to determine which plasmids had the PCR product cloned in the correct orientation relative to the *attL* sites in pCR8/GW/TOPO (Figure 8, Table 5). Plasmid 1 (Figure 8) had the *PAT16* PCR product in the correct orientation, while plasmids 2 and 3 had the insert in the reverse orientation. The *PAT16* gene in plasmid 1 was sequenced to confirm that there were no PCR errors.

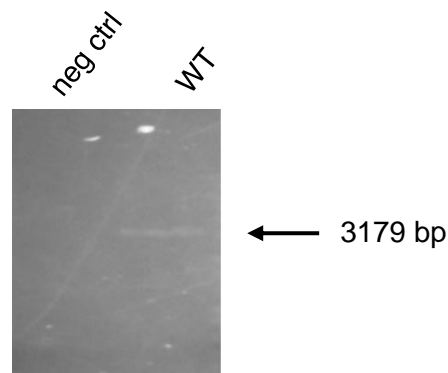


Figure 7. Amplification of *PAT16* PCR product using *PAT16*-C and p*PAT16* reverse gave product of the expected size.

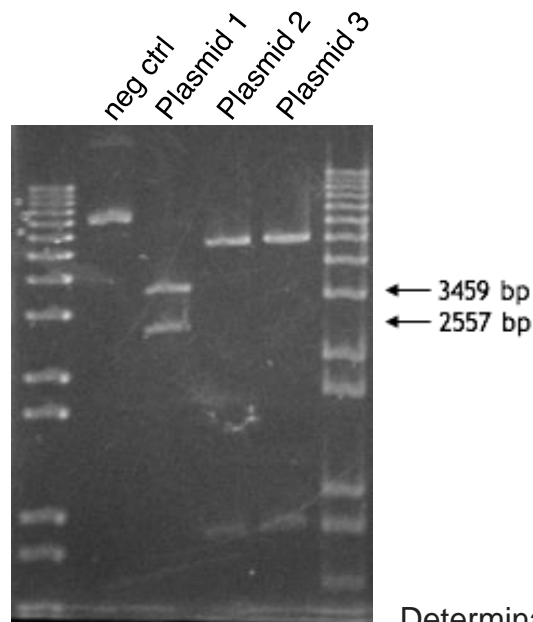


Figure 8. Determination of orientation of PCR products in pCR8/GW/TOPO with restriction digestion using EcoRV.

Table 5. Expected product sizes for restriction digests after TOPO cloning into pCR8/GW/TOPO and Gateway cloning into reporter plasmid GWB203. Gateway cloning only produces one orientation.

plasmid	restriction enzyme	correct (forward) orientation (bp)	incorrect orientation (bp)
PAT16 in pCR8/GW/TOPO	EcoRV	2557, 3459	874, 5122
PAT16 in pGWB203	PvuII	457, 1699, 1928, 4218, 5081, 5889	—
PAT16 + pGWB203	SspI	1414, 1947, 2048, 2515, 3250, 4871	—

Next, the *PAT16* region was moved from pCR8/GW/TOPO into the pGWB203 Gateway destination vector via Gateway Cloning. pGWB203 destination vector has several important components including an *HPT* hygromycin resistance gene, a chloramphenicol acetyl transferase resistance gene, a *GUS* β -glucuronidase reporter

gene, and *attR1* and *attR2* sites. These components are all found between the left and right borders⁷. The Gateway cloning reaction products were transformed into *E. coli* TOP10 cells by electroporation and the desired plasmids were selected on LB plates containing 50 µg/mL kanamycin. Six individual plasmids were isolated, purified, and quantified. Their concentrations were 23.6 ng/uL, 13.76 ng/uL, 19.1 ng/uL, 13.5 ng/uL, 32.2 ng/uL, and 11.94 ng/uL. To confirm plasmid structure, restriction digests were performed on each of the six plasmids using the restriction enzymes PvuII and SspI (Figure 9). The restriction digests of plasmids 7 and 10 showed products of the expected size using both PvuII and SspI restriction enzymes (Figure 9). The other four plasmids did not have the correct fragment patterns.

Both pGWB203-PAT16 plasmids were transferred into *Agrobacterium* GV3101 electrocompetent cells using electroporation. The transformants were streaked onto plates containing kanamycin. Individual colonies were then inoculated into LB broth containing kanamycin and grown for two days. Both pGWB203-PAT16 plasmids 7 and 10 were used for *Agrobacterium* transformation of wildtype *Arabidopsis thaliana* Columbia-0 plants. Three pots containing several flowering wildtype *Arabidopsis* plants were transformed with T-DNA from plasmid 7, and two pots of plants were transformed with T-DNA from plasmid 10 transformants.

A

24

undigested plasmid 10
Plasmid 7
Plasmid 10

B

Plasmid 7
Plasmid 10

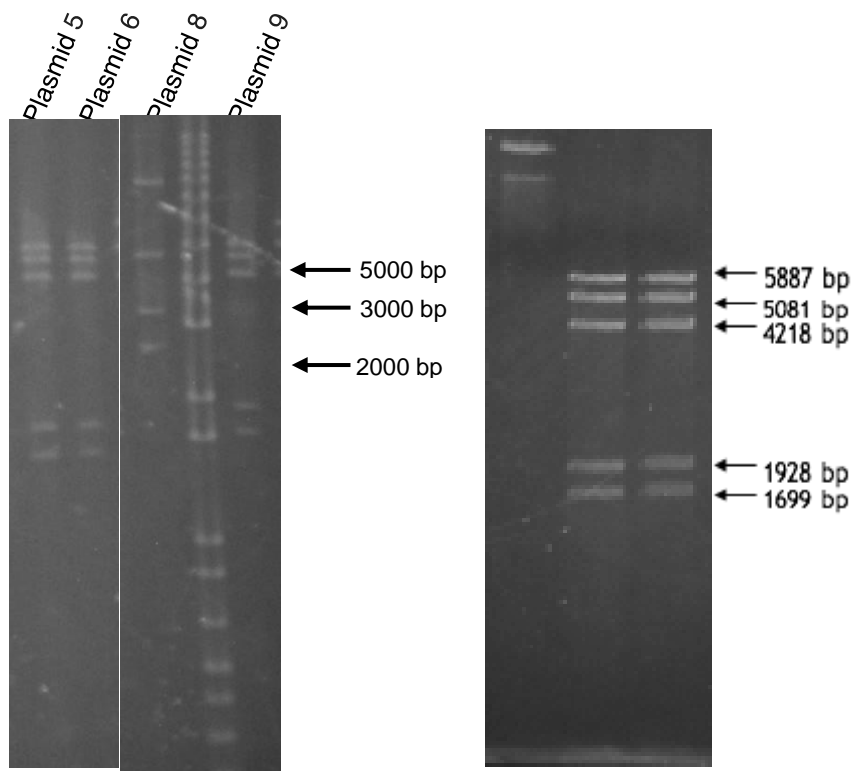


Figure 9. Agarose gels showing the expected sizes for pGWB203-PAT16 plasmids 7 and 10 using restriction enzymes A) PvuII and B) SspI.

Discussion

PAT genes are ubiquitous among eukaryotes and have been well studied in yeast, but have not been characterized extensively in plants. PATs have a relatively low level of sequence conservation, but several motifs are conserved among PAT families¹. All PATs have the essential DHHC site necessary for catalytic activity. The overarching goal of this study was to characterize palmitoyl transferase mutants using the model plant *Arabidopsis*. T-DNA mapping, mRNA transcript detection, and the GUS reporter gene system were used to characterize *pat3-2* and *pat3-3* mutants. In addition, a PAT16-GUS construct was made to analyze *PAT16* gene expression in future studies.

T-DNA mapping using PCR uncovered a partial structure of the T-DNA and of the *PAT3* gene at the site of T-DNA insertion. T-DNA mapping and sequencing of the T-DNA junctions with the genomic DNA showed that *pat3-2* and *pat3-3* are likely the same mutant. Sequencing revealed that the T-DNA was located in the cytosolic tail of *PAT3*, after the fourth transmembrane domain. The T-DNA insertion caused a 76 base pair deletion in *PAT3* in an area containing two regions that are highly conserved across Clade A PATs. The T-DNA insertion would be more advantageous if it were located at the beginning of the gene, but it could still prevent functional protein from being made in this location.

RT-PCR and GUS histochemical assays showed that *PAT3* is expressed in flowers, which is supported by microarray data on Arabidopsis eFP Browser¹³. cDNA was detected using primers upstream of and flanking the T-DNA in *pat3-2*. The amplification of products from mutant tissue samples using primers flanking the T-DNA

called into question whether *pat3-2* mutant plants are actually homozygous. Future studies should include verifying that we have a homozygous mutant before we can move forward with additional mRNA transcript detection and mutant characterization. Additionally, *pat3-3* plants should be genotyped to verify that those mutants are also homozygous. If the *pat3-2* plants are homozygous, it is possible that the T-DNA is spliced out of the primary transcript because of its location at an intron-exon junction and that is why transcript is being detected using primers flanking the insertion. Studies involving protein assays like immunodetection using antibodies instead of mRNA transcript detection could be done if this is the case.

Further future work includes isolation of *PAT16-GUS* transformed plants via hygromycin selection, collection of seeds from first generation *PAT16-GUS* plants and genotyping. GUS histochemical assays on these plants should be performed in order to characterize *PAT16* gene expression. Additional assays of *PAT3-GUS* and other *PAT-GUS* constructs would help tell a better story of *PAT* gene expression. Characterization of *PAT* mutants helps us determine if mutants are knockouts before we search for a phenotype and infer the function of the gene. Mutant characterization is an essential step in studying *PAT* proteins. Utilizing *PAT* mutants in *Arabidopsis* to analyze the function and importance of *PAT* genes will help us understand the role of *PAT* genes in plants and other organisms.

References

1. Batistic O. (2012). Genomics and Localization of the Arabidopsis DHHC-Cysteine-Rich Domain S-acyltransferase Protein Family. *Plant Physiology*. 160: 1-30.
2. Qi B, Doughty J, Hooley R. (2013). A Golgi and tonoplast localized S-acyl transferase is involved in cell expansion, cell division, vascular patterning and fertility in Arabidopsis. *New Phytologist*. 200: 1-24.
3. Hemsley PA (2009). Protein S-acylation in plants. *Molecular Membrane Biology*. 26: 114–125.
4. Ohno Y, Kashio A, Ogata R, Ishitomi A, Yamazaki Y, & Kihara A. (2012). Analysis of substrate specificity of human DHHC protein acyltransferases using a yeast expression system. *Molecular Biology of the Cell*. 23: 4543–4551.
5. "About Arabidopsis." *The Arabidopsis Information Resource*, 10 July 2009, www.arabidopsis.org/portals/education/aboutarabidopsis.jsp. Accessed 10 May 2018.
6. Hemsley PA, Weimar T, Lilley KS, Dupree P, Grierson CS. (2013). A proteomic approach identifies many novel palmitoylated proteins in Arabidopsis. *New Phytologist* 197: 805-814.
7. Hemsley PA, Kemp AC, Grierson CS. (2005) The TIP GROWTH DEFECTIVE 1 S-acyl transferase regulates plant cell growth in *Arabidopsis*. *The Plant Cell* 17: 2554-2563.
8. Yaxiao L, Baoxi Q. (2017). Progress toward Understanding Protein S-Acylation: Prospective in Plants." *Frontiers in Plant Science* 8: 346. PMC. Web. 17 May 2018.
9. Klimyuk K, Carroll B, Thomas C, Jones J. (1993). Alkali treatment for rapid preparation of plant material for reliable PCR analysis. *The Plant Journal*. 3: 493-494.
10. Nakagawa T, Kurose T, Hino T, Tanaka K, Kawamukai M, Niwa Y, Toyooka K, Matsuoka K, Jinbo T, and Kimura T. (2007). Development of a series of gateway binary vectors, pGWBs, for realizing efficient construction of fusion genes for plant transformation. *Journal of Bioscience and Bioengineering*. 104: 34-41.
11. Martin T, Wöhner R-V, Hummel S, Willmitzer L, Frommer WB. (1992). The GUS reporter system as a tool to study plant gene expression. *In GUS Protocols: Using the GUS Gene as a Reporter of Gene Expression*. (S Gallagher, ed.), Academic Press, NY.
12. Ulker B, Peiter E, Dixon D, Moffat C, Capper R, Bouche N, Edwards R, Sanders D, Knight H, Knight R. (2008). Getting the most out of publicly available T-DNA insertion lines. *The Plant Journal*. 56: 665-677.
13. Winter D, Vinegar B, Nahal H, Ammar R, Wilson GV, Provart NJ. (2007) An "Electronic Fluorescent Pictograph" Browser for Exploring and Analyzing Large-Scale Biological Data Sets. *PLoS ONE* 2(8): e718. <https://doi.org/10.1371/journal.pone.0000718>